Stereoselectivity in a Chiral Ruthenium Ethylene Hydride Complex: Evidence of an Agostic Intermediate

J. W. Faller* and Philip P. Fontaine

Yale University, P.O. Box 208107, New Haven, Connecticut 06520-8107

Received September 22, 2006

Treatment of Ru(η^6:η^1-$Me_2NC_6H_4C_6H_4PCy_2$)Cl_2 with MeLi resulted in the formation of Ru(η^6:η^1-$Me_2NC_6H_4C_6H_4PCy_2$)Me_2, which reacted with Ph_3CPF_6 to form the cationic olefin hydride complex [Ru(η^6:η^1-$Me_2NC_6H_4C_6H_4PCy_2$)($H_2C{=}CH_2$)(H)]PF_6. The new complexes were characterized by spectroscopy and by X-ray crystallographic analysis. The diastereomeric olefin hydride complexes were observed to exhibit two fluxional processes: a facile olefin rotation and another process that results in the exchange of the hydride and olefin protons. As the rate of diastereomer interconversion is much slower than that of olefin insertion, our studies suggest that the latter exchange takes place through an agostic species which undergoes dynamic methyl rotation.

Introduction

The insertion of olefins into metal−hydride bonds is of fundamental importance to several catalytic processes, including olefin hydrogenations, isomerizations, and hydroformylations. The barrier for olefin insertion into a metal−hydride bond is generally quite low, lower than that for their insertion into a metal−alkyl bond. Therefore, olefin hydride complexes are less common than olefin alkyl complexes. Nevertheless, there are a number of reported olefin hydride complexes, including those with the olefin and hydride bound in a *cis* relationship. Such olefin hydride complexes of several metals (Mo,[1] Co,[2−4] Rh,[2,3,5,6] Ir,[7] Os,[7] Ru,[7−13] Pt,[14] Nb,[15] and Ta[16]) are known, most of which undergo reversible migratory insertion/β-hydride elimination processes. For the ruthenium variants, however, there are only three reported cases of a reversible migratory insertion process.[9−11] Closely related to the classical, terminal hydride complexes are the complexes containing a three-center−two-electron C−H−M bond (an agostic interaction). There have also been many reports of agostic ethyl species,[5,17−38] and their importance in polymerization reactions has been noted on several occasions.[5,24,29,35,39,40]

Owing to their anticipated tolerance of polar functional groups, ruthenium complexes are sought which are capable of

(1) Byrne, J. W.; Blaser, H. U.; Osborn, J. A. *J. Am. Chem. Soc.* **1975**, *97*, 3871−3873.
(2) Brookhart, M.; Lincoln, D. M. *J. Am. Chem. Soc.* **1988**, *110*, 8719−8720.
(3) Schmidt, G. F.; Brookhart, M. In *J. Am. Chem. Soc.* **1985**, *107*, 1443−1444.
(4) Klein, H. F.; Hammer, R.; Gross, J.; Schubert, U. *Angew. Chem., Int. Ed. Engl.* **1980**, *19*, 809−810.
(5) Brookhart, M.; Hauptman, E.; Lincoln, D. M. *J. Am. Chem. Soc.* **1992**, *114*, 10394−10401.
(6) Werner, H.; Feser, R. *J. Organomet. Chem.* **1982**, *232*, 351−370.
(7) Werner, H.; Kletzin, H.; Hohn, A.; Paul, W.; Knaup, W.; Ziegler, M. L.; Serhadli, O. *J. Organomet. Chem.* **1986**, *306*, 227−239.
(8) Kletzin, H.; Werner, H.; Serhadli, O.; Ziegler, M. L. *Angew. Chem., Int. Ed. Engl.* **1983**, *22*, 46−47.
(9) Faller, J. W.; Chase, K. J. *Organometallics* **1995**, *14*, 1592−1600.
(10) Yi, C. S.; Lee, D. W. *Organometallics* **1999**, *18*, 5152−5156.
(11) Umezawa-Vizzini, K.; Lee, T. R. *Organometallics* **2004**, *23*, 1448−1452.
(12) Werner, H.; Werner, R. *J. Organomet. Chem.* **1979**, *174*, C63−C66.
(13) Lindner, E.; Pautz, S.; Fawzi, R.; Steimann, M. *Organometallics* **1998**, *17*, 3006−3014.
(14) Chatt, J.; Coffey, R. S.; Gough, A.; Thompson, D. T. *J. Chem. Soc. A* **1968**, 190.
(15) Doherty, N. M.; Bercaw, J. E. *J. Am. Chem. Soc.* **1985**, *107*, 2670−2682.
(16) Burger, B. J.; Santarsiero, B. D.; Trimmer, M. S.; Bercaw, J. E. *J. Am. Chem. Soc.* **1988**, *110*, 3134−3146.
(17) Brookhart, M.; Green, M. L. H. *J. Organomet. Chem.* **1983**, *250*, 395−408.
(18) Brookhart, M.; Green, M. L. H.; Pardy, R. B. A. *J. Chem. Soc., Chem. Commun.* **1983**, 691−693.
(19) Dawoodi, Z.; Green, M. L. H.; Mtetwa, V. S. B.; Prout, K. *J. Chem. Soc., Chem. Commun.* **1982**, 802−803.
(20) Fellmann, J. D.; Schrock, R. R.; Traficante, D. D. *Organometallics* **1982**, *1*, 481−484.
(21) Kazlauskas, R. J.; Wrighton, M. S. *J. Am. Chem. Soc.* **1982**, *104*, 6005−6015.
(22) Cracknell, R. B.; Orpen, A. G.; Spencer, J. L. *J. Chem. Soc., Chem. Commun.* **1984**, 326−328.
(23) Cracknell, R. B.; Orpen, A. G.; Spencer, J. L. *J. Chem. Soc., Chem. Commun.* **1986**, 1005−1006.
(24) Schmidt, G. F.; Brookhart, M. *J. Am. Chem. Soc.* **1985**, *107*, 1443−1444.
(25) Yang, G. K.; Peters, K. S.; Vaida, V. *J. Am. Chem. Soc.* **1986**, *108*, 2511−2513.
(26) Benn, R.; Holle, S.; Jolly, P. W.; Mynott, R.; Romao, C. C. *Angew. Chem., Int. Ed. Engl.* **1986**, *25*, 555−556.
(27) Brookhart, M.; Lincoln, D. M.; Volpe, A. F.; Schmidt, G. F. *Organometallics* **1989**, *8*, 1212−1218.
(28) Thompson, M. E.; Baxter, S. M.; Bulls, A. R.; Burger, B. J.; Nolan, M. C.; Santarsiero, B. D.; Schaefer, W. P.; Bercaw, J. E. *J. Am. Chem. Soc.* **1987**, *109*, 203−219.
(29) Brookhart, M.; Volpe, A. F.; Lincoln, D. M. *J. Am. Chem. Soc.* **1990**, *112*, 5634−5636.
(30) Alelyunas, Y. W.; Guo, Z. Y.; Lapointe, R. E.; Jordan, R. F. *Organometallics* **1993**, *12*, 544−553.
(31) Etienne, M. *Organometallics* **1994**, *13*, 410−412.
(32) Etienne, M.; Biasotto, F.; Mathieu, R.; Templeton, J. L. *Organometallics* **1996**, *15*, 1106−1112.
(33) Fryzuk, M. D.; Johnson, S. A.; Rettig, S. J. *J. Am. Chem. Soc.* **2001**, *123*, 1602−1612.
(34) Jaffart, J.; Etienne, M.; Maseras, F.; McGrady, J. E.; Eisenstein, O. *J. Am. Chem. Soc.* **2001**, *123*, 6000−6013.
(35) Shultz, L. H.; Brookhart, M. *Organometallics* **2001**, *20*, 3975−3982.
(36) Clegg, W.; Eastham, G. R.; Elsegood, M. R. J.; Heaton, B. T.; Iggo, J. A.; Tooze, R. P.; Whyman, R.; Zacchini, S. *Organometallics* **2002**, *21*, 1832−1840.
(37) Wiencko, H. L.; Kogut, E.; Warren, T. H. *Inorg. Chim. Acta* **2003**, *345*, 199−208.
(38) Oulie, P.; Brefuel, N.; Vendier, L.; Duhayon, C.; Etienne, M. *Organometallics* **2005**, *24*, 4306−4314.
(39) Margl, P.; Deng, L. Q.; Ziegler, T. *Organometallics* **1998**, *17*, 933−946.
(40) Thorshaug, K.; Stovneng, J. A.; Rytter, E. *Macromolecules* **2000**, *33*, 8136−8145.

10.1021/om060868j CCC: $37.00
Publication on Web 02/23/2007

Scheme 1. Synthesis of 2 and 3

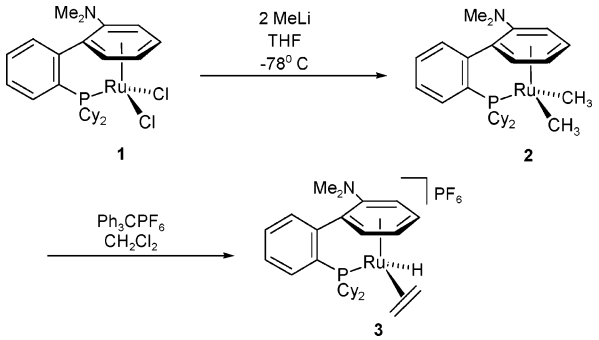

catalyzing Ziegler−Natta type polymerizations. Despite this, there have only been a few reported ruthenium-catalyzed polymerizations, and these have been restricted to ethylene.[41−43] If such a catalyst were chiral, the added advantage of stereoselective polymerization would become feasible. On this basis, and given the applicability of other olefin hydride complexes to polymerization catalysis, we set out to prepare and study the dynamics of a novel chiral ruthenium ethylene hydride complex. The diastereomeric nature of this complex provides an insight into the nature of the unobserved ethyl intermediate that is formed. Thus, this report details the facile conversion of the planar-chiral arene-tethered complex Ru(η^6:η^1-$Me_2NC_6H_4C_6H_4$-PCy_2)Cl_2 (**1**) into the dimethyl analogue Ru(η^6:η^1-Me_2-$NC_6H_4C_6H_4PCy_2$)Me_2 (**2**), which is then in turn converted to [Ru(η^6:η^1-$Me_2NC_6H_4C_6H_4PCy_2$)($H_2C{=}CH_2$)(H)]PF_6 (**3**) upon the addition of CPh_3PF_6. The synthesis of the chiral-at-metal **3** is stereoselective, with one of the isomers present in 86% diastereomeric excess (de). The solid-state structure shows that the η^2-ethylene ligand is bound in the *anti* position relative to the NMe_2 group in the preferred diastereomer. NMR studies in solution have suggested that two low-barrier dynamic processes are occurring: an olefin rotation and an "in-place" methyl rotation of an agostic intermediate.

Results and Discussion

The treatment of **1** with an excess of MeLi results in conversion to the dimethyl analogue **2** in high yield (Scheme 1). This neutral complex is moderately stable and extremely soluble in most organic solvents, including hydrocarbons. Although crystals were not readily obtained, the X-ray structure was obtained from a single crystal that was produced by slow diffusion of Et_2O into a benzene solution of **2**. The structure (Figure 1) shows the Ru−C_{Me} distances to be very similar (2.137 and 2.144 Å) and much shorter with respect to the Ru−Cl distances in **1** (2.401 and 2.419 Å). The Ru−P distance is also slightly shorter for **2** than for **1**.[44] The diastereotopic nature of the two methyl groups is evidenced by NMR, as the ^{1}H NMR spectrum shows two doublets at δ 0.91 and 0.63 ($^3J_{H-P}$ = 5.2 Hz) and the ^{13}C NMR spectrum shows two doublets at δ −10.9 and −11.1 ($^2J_{C-P}$ = 4−5 Hz).

The dimethyl complex **2** is readily converted to Ru(η^6:η^1-$Me_2NC_6H_4C_6H_4PCy_2$)($H_2C{=}CH_2$)(H)]PF_6 (**3**) upon the addition of CPh_3PF_6 (Scheme 1). This reaction, which has been observed for other ruthenium and osmium arene complexes, is believed

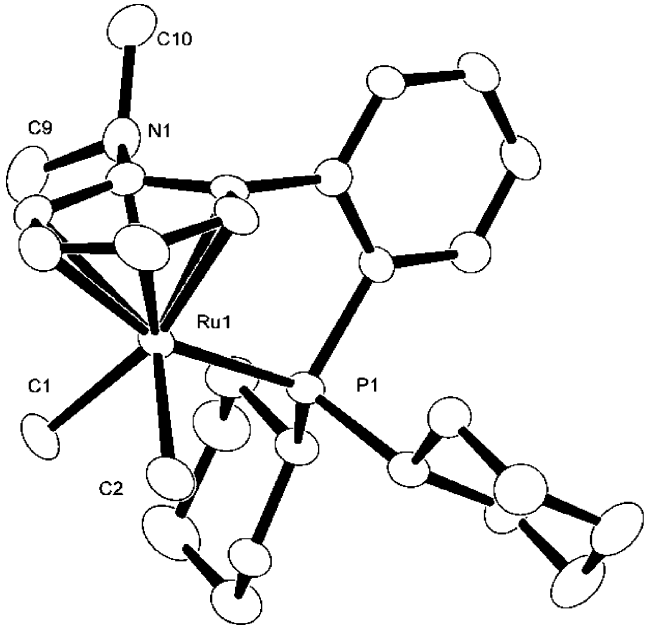

Figure 1. ORTEP diagram of (*S*)-**2**.

Scheme 2. Proposed Mechanism for Formation of 3

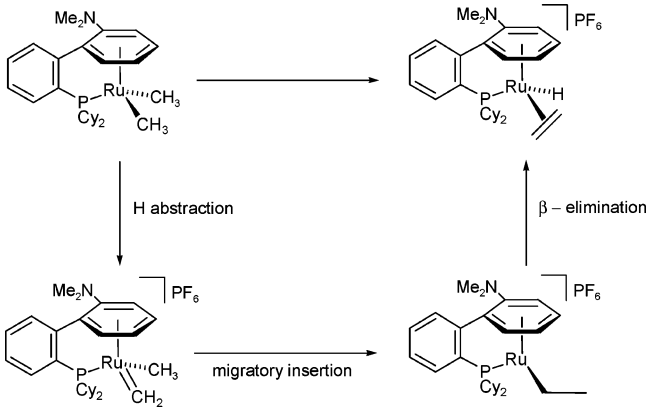

to be initiated by hydrogen abstraction from one of the methyl groups, forming a transient carbene species that undergoes an insertion of the remaining methyl group, furnishing a 16-electron ethyl intermediate. The formation of the ethylene hydride complex would then result from a β-hydride elimination of this ethyl species (Scheme 2).[8,11] The room-temperature ^{1}H NMR of **3** shows a sharp and well-separated doublet at δ −8.61, suggestive of a terminal hydride and not an agostic interaction. The strong coupling through the metal center to the phosphorus ($^2J_{H-P}$) of 38.9 Hz corroborates this interpretation.[5]

As **3** is both planar-chiral and chiral-at-metal, two diastereomers are possible. Indeed, while the synthesis of **3** results in the preferential formation of one of these isomers, a small amount (7%) of a minor isomer is observed. We have observed in our prior work with this arene-tethered system that the planar chiral ligand can exert a strong influence on controlling the metal-centered chirality.[44,45] Crystals suitable for X-ray diffraction were obtained by slow diffusion of Et_2O into a CH_2Cl_2 solution of **3**, and the solid-state structure shows the η^2-ethylene is bound *anti* with respect to the NMe_2 group (Figure 2). This isomer is expected to be the more stable of the two, as follows from our previous studies that have shown the ability of the NMe_2

(41) James, B. R.; Markham, L. D. *J. Catal.* **1972**, *27*, 442-&.
(42) Komiya, S.; Yamamoto, A.; Ikeda, S. *Bull. Chem. Soc. Jpn.* **1975**, *48*, 101−107.
(43) Nomura, K.; Warit, S.; Imanishi, Y. *Macromolecules* **1999**, *32*, 4732−4734.
(44) Faller, J. W.; D'Alliessi, D. G. *Organometallics* **2003**, *22*, 2749−2757.
(45) Faller, J. W.; Fontaine, P. P. *Organometallics* **2005**, *24*, 4132−4138.

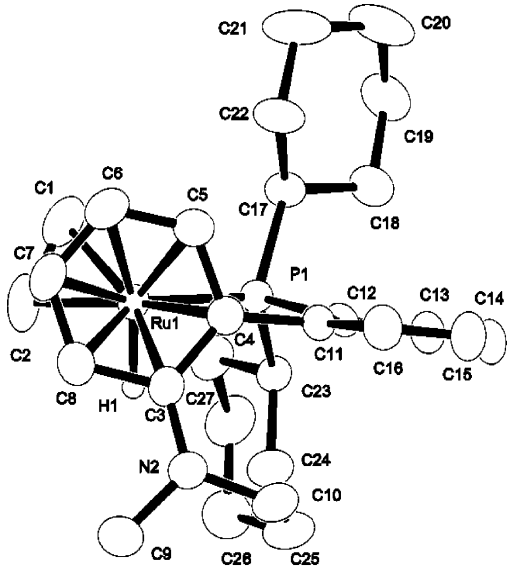

Figure 2. ORTEP diagram of (S_{Ru},*R*)-**3**.

Table 1. Selected Distances and Angles for 3

molecule 1		molecule 2	
	Distances (Å)		
Ru−H1	1.48(3)	Ru−H1	1.52(3)
Ru−C1	2.172(3)	Ru−C1	2.188(3)
Ru−C2	2.176(3)	Ru−C2	2.190(3)
Ru−P1	2.2894(9)	Ru−P1	2.2866(9)
C1−C2	1.398(5)	C1−C2	1.395(5)
C2−H1[a]	2.23	C2−H1[a]	2.31
	Angles (deg)		
H1−Ru−P1	78(1)	H1−Ru−P1	79(1)
C1−Ru−P1	91.79(11)	C1−Ru−P1	91.66(10)
C2−Ru−P1	108.01(10)	C2−Ru−P1	107.22(10)

[a] These distances correspond to through-space distances, not bond lengths.

substituent to direct the larger ligand into the *anti* binding site, owing to the unfavorable steric interactions that would result from *syn* coordination.

The X-ray analysis showed that **3** crystallized in the $P2_1/c$ space group, with two molecules in the asymmetric unit cell. The differences between the two molecules are very minor, differing in the conformations of the cyclohexyl groups, and only slight variations are observed in the bond lengths and angles (Table 1). The structure shows that the η^2-ethylene is in fact disposed nearly *trans* to the phosphine. Whereas the accuracy associated with the location of hydrides by X-ray analysis is low, the position of the hydride could be refined and appears to be in unusually close proximity to the phosphine; the latter is evidenced from the small P−Ru−H bond angle (78 and 79° for the respective molecules). The C−Ru bonds for the η^2-ethylene ligand are essentially equivalent in both molecules (2.172 and 2.176 Å in one case and 2.188 and 2.190 Å for the other), illustrating that the bonding to the olefin ligand is not significantly asymmetric. The observed Ru−H distances (1.52 and 1.48 Å, respectively, but perhaps longer in reality) are somewhat shorter than is usually observed, although an even shorter Ru−H distance (1.44 Å) has been reported.[11] The C−C bond distances of the η^2-ethylene ligand are 1.398 and 1.395 Å for the two molecules, and the distances from the hydride to the adjacent carbon are 2.308 and 2.232 Å, respectively. Therefore, the solid-state structure, like the solution structure, appears to be a classical olefin hydride complex and not an agostic ethyl complex.

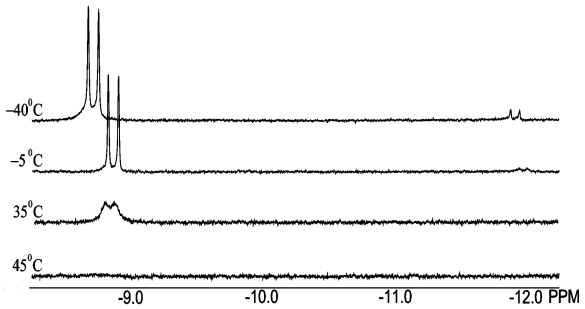

Figure 3. Dynamic NMR of Hydride Region.

The room-temperature ^{1}H and ^{13}C NMR of **3** shows that there is a fast rotation of the ethylene ligand, as evidenced by the appearance of two olefinic proton resonances and one olefinic carbon resonance. As these ^{1}H NMR resonances are broad at room temperature, the temperature was lowered, which resulted in their sharpening. The low barrier associated with this process was demonstrated by lowering the temperature to −80 °C, at which point no decoalescence had occurred and there were still two sharp resonances apparent. Therefore, the line broadening at room temperature is due to another dynamic process. As previously mentioned, at room temperature a doublet hydride resonance at δ −8.61 is apparent in the ^{1}H NMR spectrum. Closer examination revealed that this resonance is actually slightly broad at room temperature. Cooling of the sample produced sharpening of the resonance, and at −40 °C another hydride resonance became apparent. This minor hydride resonance corresponds to the minor isomer of **3**, which is too broad to be observed in the room-temperature spectrum (Figure 3). The line broadening in the hydride resonances and the olefin resonances is related, as was determined with an EXSY spectrum, which showed cross-peaks between the olefin and hydride resonances, as well as between the two olefinic proton resonances for the major isomer. That each of the five protons, four from the ethylene ligand and the hydride, are exchanging is indicative of the fast olefin rotation relative to a second dynamic process that involves both the hydride and the olefin ligand.

The simplest possibility is a reversible migratory insertion process, which would give rise to a 16-electron ethyl intermediate and which would allow the permutations of the observed exchange process. A question arises, then, as to whether or not two such diastereomers of **3** are able to interconvert, since the intermediate of the migratory insertion process should provide a pathway for the interconversion of the isomers. That is, the inversion barriers for 16-electron arene ruthenium complexes are believed to be quite low, generally substantially below 15 kcal/mol,[46] and so the epimerization of the metal should be a very facile process if there were an equilibrium with a 16-electron ethyl species. It should be noted that such an ethyl species, which is depicted as being pyramidal in Scheme 3, could also have a planar geometry, as the ground-state geometries of 16-electron half-sandwich complexes are very sensitive to the ligand architecture.[46] In either case, the most important feature is that an equilibrium with a 16-electron complex containing a normal σ-bonded ethyl group should provide a path for a rapid epimerization.

No exchange was observed between the two diastereomers in EXSY spectra. In addition, the interconversion of the two diastereomers would result in the broadening of all of the resonances in the NMR spectrum. However, only the olefin and

(46) Ward, T. R.; Schafer, O.; Daul, C.; Hofmann, P. *Organometallics* **1997**, *16*, 3207−3215.

Scheme 3. Interconversion of Diastereomers of 3 via a Pyramidal Ethyl Species

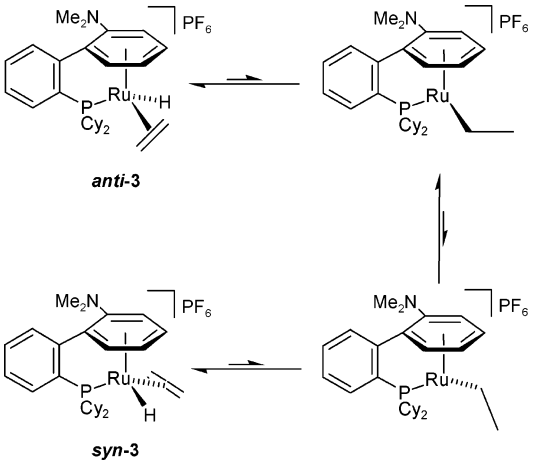

hydride resonances become broad, while the remaining resonances for the distinct diastereomers remain sharp throughout the dynamic temperature range (up to 75 °C, indicating a barrier of >20 kcal mol^{-1} for the interconversion of the two isomers). The free energies of activation for the dynamic processes of **3** were calculated from the line broadening in the ^{1}H NMR spectrum. For the major isomer, a barrier ($\Delta G^{\ddagger}$) of 15.2 kcal/mol was calculated, while for the minor isomer $\Delta G^{\ddagger} = 13.0$ kcal/mol. This corresponds to rates of 40 and 176 s^{-1} at 25 °C, respectively, and therefore, the calculated ratio of rates is only 4.4:1, while the ratio of concentrations of isomers is ~13:1. Furthermore, crystallization provides crystals of a single isomer, as shown in Figure 2. The NMR spectrum taken *immediately* upon dissolution of the crystals shows a preponderance of a single isomer (~98%) which equilibrated with a half-life on the order of 10 min, indicating an epimerization barrier of ~22 kcal mol^{-1}. (Owing to the small percentage of the minor isomer an accurate value for the barrier was not obtained.) In any case, it is clear from all this evidence that the dynamic processes observed by NMR *are not* leading to the rapid interconversion of the two diastereomers.

In order to account for these observations, we propose an equilibrium between the terminal ethylene hydride complex and an *agostic ethyl species*, rather than a 16-electron species with a normal σ-bound ethyl group. This accounts for the observed lack of interconversion between the two diastereomers, since the agostic interaction avoids the coordinative unsaturation that would lead to fast epimerization. Also, these proposed intermediates can still give rise to the exchange of the olefin and hydride protons, through an "in-place walking" mechanism in which the methyl group retains contact with the metal center throughout the dynamic process.[5,27,47−49] This process (Figure 4), when coupled with the faster olefin rotation, would lead to the exchange behavior observed in the present case. It should be noted that the formation of a true 16-electron σ-ethyl intermediate cannot be unequivocally ruled out. For example, if the formation of such an intermediate had a high energy approaching that of the transition state, then similar rates might be observed. Nevertheless, upon consideration of other analyses[3] of this type of problem, we feel the more likely explanation of the high

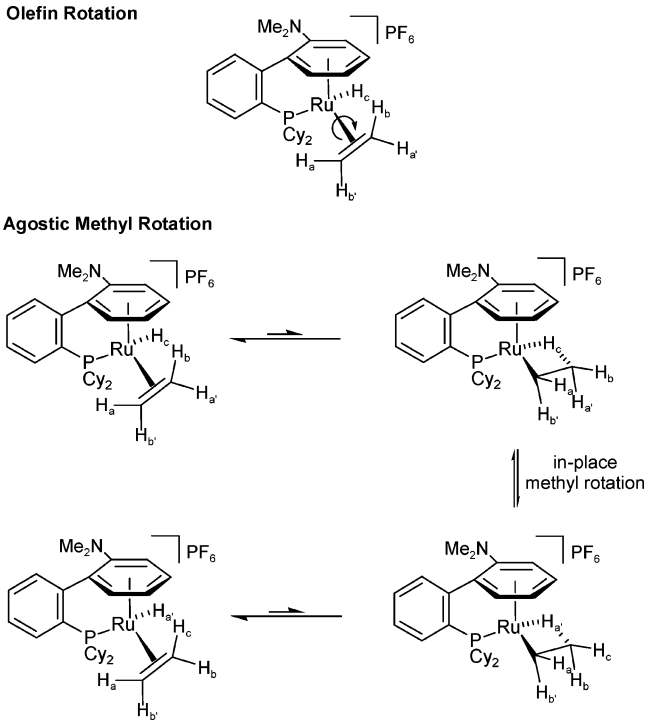

Figure 4. Dynamic Behavior of **3**.

barrier for epimerization involves an agostic rather than a 16-electron species.

The processes discussed here have analogues in the $[(C_5H_5)(L)Co-CH_2CH_2-H]^+$ case studied by Brookhart *et al.*, who have proposed that, for agostic complexes that exhibit such dynamic behavior, it is usually the case that the isomerization of the metal complex *via* a 16-electron ethyl intermediate is significantly slower than both olefin rotation and methyl rotation.[27] The cobalt complexes differ in that the agostic ethyl is the stable form, rather than the ethylene hydride found for **3.** The situation is that it is often difficult to distinguish between the processes; that is, dynamic methyl rotation of an agostic interaction versus migratory insertion to yield a 16-electron ethyl species versus inversion at the metal center. One exception is the report by Spencer *et al.*, in which the rate of inversion of the metal chirality, stemming from the formation of a 16-electron ethyl intermediate, was directly measured by following the averaging of diastereotopic methyl groups with L = Me_2PPh by NMR.[23] In Spencer's case it was also observed that the formation of the 16-electron ethyl and inversion of the cobalt metal center was a higher barrier process (13.4 kcal mol^{-1}) than the process which resulted in the exchange of terminal and bridging methyl resonances (9.6 kcal/mol). One should note that it is also difficult to disentangle the actual rate of inversion of a pyramidal intermediate from the rate of formation of the 16-electron pyramidal intermediate. Hence, the barrier to inversion could be a component of the total. Brookhart determined an inversion barrier of ~3 kcal mol^{-1} in an analogous case.[27] In the present case, the planar chirality of the arene-tethered ligand makes the overall inversion process easily distinguishable from the other processes. Specifically, olefin rotation has a very low barrier and the formation of an agostic species does not result in the epimerization of **3**, whereas the formation of a normal σ-ethyl intermediate would provide a rapid epimerization route.

Conclusions

The planar chiral dichloride complex **1** has been converted into the dimethyl analogue **2**, which was subsequently converted

(47) Green, M. L. H.; Wong, L. L. *J. Chem. Soc., Chem. Commun.* **1988**, 677−679.

(48) Bercaw, J. E.; Burger, B. J.; Green, M. L. H.; Santarsiero, B. D.; Sella, A.; Trimmer, M. S.; Wong, L. L. *J. Chem. Soc., Chem. Commun.* **1989**, 734−736.

(49) Casey, C. P.; Yi, C. S. *Organometallics* **1991**, *10*, 33−35.

into a cationic ethylene hydride complex **3**. The latter reaction is stereoselective, as the product **3** forms in 86% de. The identity of both derivatives has been established by ^{1}H, ^{31}P, and ^{13}C NMR, along with X-ray crystallography. The metal-centered chirality in **3** is effectively controlled by the planar chirality of the arene-tethered ligand and, more specifically, the directing influence of the NMe_2 group. Both the solid-state and solution structures are suggestive of a classical, terminal hydride species. However, the two diastereomers of **3** were seen to undergo a dynamic process, with the barriers being 15.2 and 13.0 kcal/mol for the major and minor species, respectively, which resulted in the exchange of the hydride and olefin resonances in the ^{1}H NMR spectrum. It was observed that the diastereomers of **3** do not interconvert *via* the dynamic processes observed by line broadening in the NMR, which is suggestive of an equilibrium involving an agostic species. If a conventional 16-electron ethyl species were involved, we would anticipate a barrier less than the >22 kcal/mol we observe. That is, the continual agostic contact to the ruthenium should slow the epimerization of the metal center. We propose, then, that the aforementioned dynamic NMR observations represent the barriers to the dynamic methyl group rotation of an agostic interaction. Thus, this is an unusual case where the barrier of such a process could be directly determined, as the diastereomers observed in this system allow for the various dynamic processes to be readily distinguishable.

Table 2. Crystallographic Data

	2	**3**
color, shape	yellow, block	yellow, block
empirical formula	$C_{28}H_{42}NPRu$	$C_{28}H_{41}F_6NP_2Ru$
formula wt	524.69	668.65
Mo Kα radiation/Å	0.710 73	0.710 73
T/K	173	173
cryst syst	monoclinic	monoclinic
space group	$P2_1/c$ (No. 14)	$P2_1/c$ (No. 14)
unit cell dimens		
a/Å	9.9085 (2)	13.1073(2)
b/Å	10.7654(2)	22.3257(3)
c/Å	24.0370(5)	20.0334(3)
β/deg	96.192(2)	94.5439(9)
V/Å^3	2549.04(8)	5843.94(13)
Z	4	8
D_{calcd}/g cm^{-3}	1.367	1.520
μ/cm^{-1} (Mo Kα)	6.93	7.03
cryst size/mm	0.10 × 0.10 × 0.10	0.12 × 0.14 × 0.24
total, unique no. of rflns	17 748, 6356	23 777, 14196
R_{int}	0.056	0.027
no. of obsd rflns ($I > 3\sigma(I)$)	4392	9329
no. of params, restraints	280, 0	709, 0
R,[a] R_w,[b] GOF	0.050, 0.063, 2.02	0.038, 0.040, 1.77
min, max resid density/e Å^{-3}	−1.98, 2.10	−0.57, 0.70

[a] $R = \sum||F_o| - |F_c||/\sum|F_o|$, for all $I > 3\sigma(I)$. [b] $R_w = [\sum[w(|F_o| - |F_c|)^2]/\sum[w(F_o)^2]]^{1/2}$.

Experimental Section

General Methods. All manipulations were carried out under a nitrogen atmosphere using standard Schlenk techniques. CH_2Cl_2 and THF were dried by distillation over CaH and Na/benzophenone, respectively, under a nitrogen atmosphere. Et_2O was dried on an alumina-based solvent purification system, and benzene was used directly without drying. MeLi and CPh_3PF_6 were used as received (Aldrich). Elemental analyses were carried out by Atlantic Microlabs. NMR spectra were recorded on a Bruker 400 MHz (operating at 162 MHz for ^{31}P and 100 MHz for ^{13}C), or a Bruker 500 MHz (operating at 202 MHz for ^{31}P and 125 MHz for ^{13}C). Chemical shifts are reported in ppm relative to solvent peaks (^{1}H), or an H_3PO_4 external standard.

Synthesis of Ru(η^6:η^1-NMe$_2$C$_6$H$_4$C$_6$H$_4$PCy$_2$)Me$_2$ (2). A flame-dried flask was charged with **1** (102 mg, 0.180 mmol) and placed under a nitrogen atmosphere. THF (5 mL) was then added, and the solution was cooled to 0 °C, before the addition of MeLi (0.60 mL, 1.6 M in Et_2O, 0.96 mmol). The resulting mixture was stirred for 30 min at this temperature and was then warmed to room temperature and stirred for an additional 30 min. The solvent was then removed under vacuum, the residue was extracted with benzene (4 × 10 mL), and the extracts were filtered through Celite. The product was dried under vacuum and used directly (85.3 mg, 90%). Anal. Calcd for $C_{28}H_{42}NPRu\cdot{}^1/_2C_6H_6$: C, 66.05; H, 8.05; N, 2.48. Found: C, 65.77; H, 8.21; N, 2.58. A crystal was obtained by slow diffusion of Et_2O into a benzene solution. ^{1}H NMR (400 MHz, C_6D_6): 7.37 (1H, m), 7.32 (1H, m), 7.09−7.04 (2H, m) (CH_{arom}); 5.22 (1H, d, J = 5.6 Hz), 5.03 (1H, d, J = 5.6 Hz), 4.87 (1H, dd, J = 5.6 Hz, 0.8 Hz), 4.49 (1H, tm, J = 5.6 Hz), (C$H_{\eta^6\text{-arene}}$); 2.50 (1H, m, C$H_{cyclohexyl}$); 2.23 (6H, s, N(CH_3)$_2$); 2.14 (1H, m, C$H_{cyclohexyl}$); 2.03−1.07 (18H, m, C$H_{2\ cyclohexyl}$); 0.99 (1H, m, C$H_{2\ cyclohexyl}$); 0.91 (3H, d, J = 5.2 Hz, Ru−CH_3); 0.63 (3H, d, J = 5.2 Hz, Ru−CH_3); 0.52 (1H, m, C$H_{2\ cyclohexyl}$). ^{13}C NMR (126 MHz, C_6D_6): 147.9 (d, J_{C-P} = 22.0 Hz, CC$_{arom}$); 147.0 (d, J_{C-P} = 35.3 Hz, CP$_{arom}$); 129.7 (CH$_{arom}$); 128.6 ($CN_{\eta^6\text{-arene}}$); 128.4, 126.8 (d, J_{C-P} = 4.7 Hz), 122.2 (CH$_{arom}$); 108.4 (d, J_{C-P} = 2.8 Hz, CC$_{\eta^6\text{-arene}}$); 97.1 (d, J_{C-P} = 3.5 Hz), 86.9 (d, J_{C-P} = 5.3 Hz), 84.6, 75.3 (d, J_{C-P} = 13.5 Hz) (CH$_{\eta^6\text{-arene}}$); 45.9 (N(CH$_3$)$_2$); 36.2 (d, J_{C-P} = 16.7 Hz), 33.1 (d, J_{C-P} = 18.9 Hz) (CH$_{cyclohexyl}$); 29.0 (d, J_{C-P} = 2.6 Hz), 28.1−27.7 (several superimposed resonances), 27.3 (d, J_{C-P} = 2.6 Hz), 27.0 (d, J_{C-P} = 2.6 Hz) (CH$_{2\ cyclohexyl}$); −10.9 (d, J_{C-P} = 4.7 Hz), −11.1 (d, J_{C-P} = 4.0 Hz) (Ru−CH$_3$). ^{31}P NMR (162 MHz): 58.0 (s).

Synthesis of [Ru(η^6:η^1-NMe$_2$C$_6$H$_4$C$_6$H$_4$PCy$_2$)(η^2-H$_2$C=CH$_2$)(H)]PF$_6$ (3). A flame-dried flask was charged with **2** (102 mg, 0.194 mmol) and CPh_3PF_6 (73.3 mg, 0.189 mmol) and placed under a nitrogen atmosphere. CH_2Cl_2 (5 mL) was added, and the solution was stirred for $^1/_2$ h, at which time it was removed and dried under vacuum. Crystals (50.2 mg, 40%) were obtained by slow diffusion of Et_2O into a CH_2Cl_2 solution of the product, performed under a nitrogen atmosphere in a Schlenk tube. Anal. Calcd for $C_{28}H_{41}F_6NP_2Ru$: C, 50.30; H, 6.18; N, 2.09. Found: C, 49.99; H, 6.20; N, 2.16. Data for the major isomer are as follows. ^{1}H NMR (500 MHz, 25 °C, CD_2Cl_2): 7.68 (1H, m), 7.54 (1H, m), 7.48 (1H, m), 7.44 (1H, d, J = 7.1 Hz), (CH$_{arom}$); 6.24 (1H, dd, J = 5.8, 1.2 Hz), 6.17 (1H, d, J = 6.9 Hz), 6.10 (1H, t, J = 5.8 Hz), 5.40 (1H, m), (C$H_{\eta^6\text{-arene}}$); 2.75 (2H, br, H_2C=CH$_2$); 2.72 (6H, s, N(CH$_3$)$_2$); 2.39 (1H, m), 2.13 (1H, m) (CH$_{cyclohexyl}$); 2.10 (2H, br, H$_2C$=CH$_2$); 1.97−0.97 (18H, m), 0.79−0.63 (2H, m) (CH$_{2\ cyclohexyl}$); −8.61 (1H, d, $^2J_{H-P}$ = 38.9 Hz, Ru−H). ^{13}C NMR (125 MHz): 145.5 (d, J_{C-P} = 17.2 Hz, CC$_{arom}$); 143.0 (d, J_{C-P} = 41.5 Hz, CP$_{arom}$); 135.7 ($CN_{\eta^6\text{-arene}}$); 131.1, 130.9, 130.3 (CH$_{arom}$); 130.2 ($CC_{\eta^6\text{-arene}}$); 128.7 (d, J_{C-P} = 6.4 Hz, CH$_{arom}$); 100.8, 96.8 (d, J_{C-P} = 6.8 Hz), 95.5, 75.3 (d, J_{C-P} = 6.4 Hz), (CH$_{\eta^6\text{-arene}}$); 43.5 (N(CH$_3$)$_2$); 36.2 (d, J_{C-P} = 19.0 Hz), 34.6 (d, J_{C-P} = 33.6 Hz), (CH$_{cyclohexyl}$); 33.7 (H$_2C$=CH$_2$); 29.4 (d, J_{C-P} = 1.6 Hz), 28.4, 28.3 (d, J_{C-P} = 6.0 Hz), 27.6 (d, J_{C-P} = 13.6 Hz), 27.4 (d, J_{C-P} = 8.2 Hz), 26.8, 26.3 (d, J_{C-P} = 13.6 Hz), 26.1, 26.0, 25.9 (CH$_{2\ cyclohexyl}$). ^{31}P NMR (162 MHz): 78.8 (s). Data for the minor isomer (observable resonances) are as follows. ^{1}H NMR (500 MHz, 25 °C, CD_2Cl_2): 6.34 (1H, t, J = 6.0 Hz), 6.16 (2H, m, superimposed by major isomer), 4.35 (1H, d, J = 6.0 Hz) (CH$_{\eta^6\text{-arene}}$); 2.79 (6H, s, N(CH$_3$)$_2$, superimposed by major isomer). ^{31}P NMR (162 MHz): 78.2 (s).

Structure Determination and Refinement. Crystals were obtained by slow diffusion of diethyl ether into a methylene chloride solution of complexes **2** and **3**. Data were collected on a Nonius KappaCCD (Mo Kα radiation) diffractometer and the data pro-

cessed with Scalepack.[50] The structures were solved by direct methods (SIR92)[51] and refined on F for all reflections.[52] Non-hydrogen atoms were refined with anisotropic displacement parameters. Hydrogen atoms were included at calculated positions. Relevant crystal and data parameters are presented in Table 2.

Structure Determination of 2. This structure determination was straightforward, and the compound had crystallized in a monoclinic cell with absences indicating a space group of $P2_1/c$.

Structure Determination of 3. This structure determination was straightforward and the compound had crystallized in a monoclinic cell with $Z = 8$ and with absences indicating a space group of $P2_1/c$, which requires two independent molecules in the asymmetric unit. The molecules are nearly identical, and only one of the cations is shown in Figure 2. One of the SbF_6 counterions showed a 3:1 disorder, which was modeled as a rotation about one F−Sb−F axis of ∼45°.

(50) Minor, W., Otwinowski, Z., Eds. HKL2000 (Denzo-SMN) Software Package. Processing of X-ray Diffraction Data Collected in Oscillation Mode. *Methods in Enzymology*; Academic Press: New York, 1997; Macromolecular Crystallography.

(51) Altomare, A.; Cascarano, G.; Giacovazzo, C.; Guagliardi, A. *J. Appl. Crystallogr*. **1993**, *26*, 343.

(52) TEXSAN for Windows version 1.06: Crystal Structure Analysis Package; Molecular Structure Corp., The Woodlands, TX, 1997−1999.

Supporting Information Available: CIF files and tables giving crystallographic data for compounds **2** and **3**. This material is available free of charge via the Internet at http://pubs.acs.org. Crystallographic data for the structural analysis have also been deposited with the Cambridge Crystallographic Data Centre: CCDC Nos. 620863 and 620862 for compounds **2** and **3**. Copies of this information may be obtained free of charge from The Director, CCDC, 12 Union Road, Cambridge CB2 1EZ, U.K. (fax, (int code) +44(1223)336-033; e-mail, deposit@ccdc.cam.ac.uk; web, www: http://www.ccdc.cam.ac.uk).

OM060868J